IJIRCCE

e-ISSN: 2320-9801 | p-ISSN: 2320-9798

INTERNATIONAL JOURNAL OF INNOVATIVE RESEARCH

IN COMPUTER & COMMUNICATION ENGINEERING

Volume 10, Issue 4, April 2022

INTERNATIONAL STANDARD SERIAL NUMBER INDIA

Impact Factor: 8.165

International Journal of Innovative Research in Computer and Communication Engineering

| e-ISSN: 2320-9801, p-ISSN: 2320-9798| www.ijircce.com | |Impact Factor: 8.165

|| Volume 10, Issue 4, April 2022 ||

| DOI: 10.15680/IJIRCCE.2022.1004168 |

Multi-Variate Predictive Loss Analysis Framework for GW-Scale Solar Cell Manufacturing: From Inline Data to Cell Efficiency Distribution

Sekhar Tatineni

Senior Director, Engineering & Production Systems Development, Singapore

ABSTRACT: The transition of silicon heterojunction solar cell manufacturing from pilot scale to multi-gigawatt volume production introduces a fundamental analytical challenge. The volume and dimensionality of inline process data generated daily at gigawatt scale far exceeds the capacity of human engineers to interpret and act upon within the timescales required to prevent yield loss. A single gigawatt-scale heterojunction cell production line generates in excess of two-point-four million individual inline measurement records per day, spanning sheet resistance, optical transmittance, carrier lifetime, implied open-circuit voltage, deposition rate, and dozens of secondary process signals. Without a systematic, automated framework for reducing this data to actionable process intelligence, the majority of this information remains latent.

This paper presents the Multi-Variate Predictive Loss Analysis framework, abbreviated herein as MPLA, a production-validated machine learning architecture developed and deployed at REC Solar's one-point-five gigawatt manufacturing facility in Singapore. The framework ingests real-time inline metrology data streams, applies a structured feature engineering and dimensionality reduction pipeline, and trains an ensemble of gradient-boosted regression models to predict final cell efficiency with a root mean square error of 0.093% absolute, derived from process data collected before the completion of cell manufacturing. The framework simultaneously decomposes predicted efficiency loss into contributions from individual process parameters, generating a continuous Pareto-ranked loss attribution that identifies the highest-impact process levers at any given time. Deployed from the eighteenth production week of 2021 onward, MPLA delivered a mean efficiency improvement of 0.37% absolute, a process capability improvement from Cpk equal to 0.84 to Cpk equal to 1.67 for the primary TCO deposition process, and a top-bin yield increase of 2.1% at the 24.8% efficiency threshold. The commercial value, calculated at one gigawatt production scale, is estimated at approximately 11.4 million dollars annually.

KEYWORDS: Predictive Analytics · Loss Analysis · Machine Learning · HJT Solar Cells · GW-Scale Manufacturing · XGBoost · Feature Engineering · Inline Metrology · Process Control · Cell Efficiency Distribution · Pareto Analysis

I. INTRODUCTION

Manufacturing intelligence, the capacity to translate raw process sensor data into predictive insight about product quality, has long been recognized as a decisive competitive lever in semiconductor fabrication. The complexity of multi-step processes and the high value density of products make data-driven yield management economically essential in chip manufacturing. The photovoltaic manufacturing industry, historically characterized by simpler process flows and lower data intensity than semiconductor backend operations, is undergoing a rapid transformation toward comparable analytical sophistication as heterojunction cell efficiency targets push toward the practical limits of silicon-based photovoltaics. Gigawatt-scale production volumes create an information environment of equivalent complexity to a leading-edge chip fabrication facility.

At REC Solar's Singapore manufacturing site, the heterojunction cell production line encompasses four process steps, from wafer Texture through, plasma-enhanced chemical vapor deposition of amorphous silicon layers, transparent conductive oxide sputtering and metallization. Each step is instrumented with multiple inline metrology tools collecting measurement data at wafer-level cadence. By early 2021, the cumulative data infrastructure of the production line was generating approximately 2.4 million measurement records per day and approximately 175 GB of raw metrology data per week. The existing process engineering capability to manually analyze and act on this data was estimated to cover

| e-ISSN: 2320-9801, p-ISSN: 2320-9798| www.ijircce.com | |Impact Factor: 8.165

|| Volume 10, Issue 4, April 2022 ||

| DOI: 10.15680/IJIRCCE.2022.1004168 |

fewer than 12% of the available parameter channels on a continuous basis. The remaining 88% of process data was archived but never actively used for efficiency optimization.

The commercial motivation for closing this analysis gap is direct and quantifiable. In a production environment operating at a gigawatt annual capacity with a mean cell efficiency of 24.5% and a top-bin yield of 18.2% at the 24.8% threshold, a single percentage point improvement in top-bin yield translates to approximately 10MW of additional high-value product annually. This is equivalent to 6.7 million dollars in incremental revenue at prevailing module pricing. The ability to identify, rank, and act on efficiency loss drivers faster and more comprehensively than traditional engineering methods is therefore a capability with direct first-order financial consequences, not merely an academic exercise in data science.

"In a GW-scale HJT manufacturing environment, the question is never whether the data contains the answer to the efficiency loss problem. It always does. The question is whether the analytical infrastructure exists to find it before the production week ends."

This paper is organized as follows. Section two reviews the data environment and metrology infrastructure at the REC Solar heterojunction production facility. Section three presents the MPLA framework architecture, model design, and training methodology. Section four describes the feature importance analysis and loss decomposition results. Section five documents the model validation performance. Section six presents the production deployment results and efficiency impact. Section seven discusses the broader implications for gigawatt-scale manufacturing analytics. Section eight concludes with key findings and future directions.

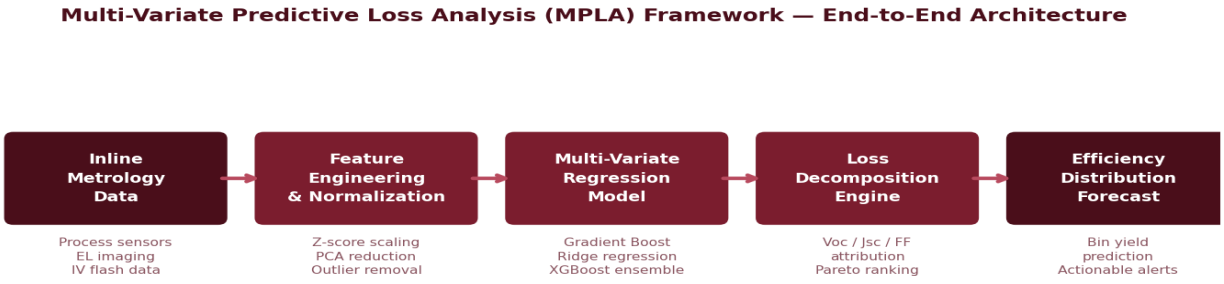

Figure 1. *End-to-end architecture of the MPLA framework, from raw inline metrology data ingestion through feature engineering, ensemble model training, loss decomposition, and efficiency distribution forecasting. The five-stage pipeline operates continuously on production data streams, generating alerts and actionable process recommendations in near real time.*

II. PRODUCTION DATA ENVIRONMENT AND METROLOGY INFRASTRUCTURE

2.1 Inline Measurement System Architecture

The metrology infrastructure supporting the MPLA framework at REC Solar Singapore was designed and deployed over the period 2018 to 2020 as part of a systematic manufacturing digitalization program. The system consists of 23 distinct inline measurement stations distributed across the cell production flow. Each measurement station is connected to a central manufacturing execution system database via an OPC-UA industrial protocol interface. Every production wafer that passes through the line receives a unique wafer identifier assigned at the incoming quality inspection gate, which is used to link all subsequent measurement records across all metrology stations into a complete per-wafer data record. This relational structure enables the MPLA framework to train on complete process-to-outcome chains rather than aggregated lot-level statistics.

The primary inline measurement channels exploited by the MPLA framework span all major process steps. At the plasma-enhanced chemical vapor deposition step, in-situ ellipsometry monitors film thickness and refractive index in real time during deposition. At the transparent conductive oxide deposition step, four-point probe sheet resistance mapping at 49 points per wafer provides spatial uniformity data in addition to mean values. Optical transmission spectrophotometry from 300 to 1200 nanometers captures the wavelength-resolved transmittance profile of the indium tin oxide film. At the screen-printing metallization step, vision-based linewidth measurement records the as-printed silver grid geometry. Photoluminescence imaging after passivation deposition captures the spatial carrier lifetime map before metallization.

| e-ISSN: 2320-9801, p-ISSN: 2320-9798| www.ijircce.com | |Impact Factor: 8.165

|| Volume 10, Issue 4, April 2022 ||

| DOI: 10.15680/IJIRCCE.2022.1004168 |

The final inline measurement prior to standard test condition flash testing is implied open-circuit voltage by quasi-steady-state photoconductance, which serves simultaneously as a process quality gate and as the highest-correlation single-variable predictor of final cell efficiency in the MPLA model.

2.2 Data Volume and Quality Characterization

The raw data environment presents several analytical challenges that must be addressed before model training can produce reliable predictions. Missing value rates across the 78 parameter channels range from 0.02% for primary metrology stations with high-reliability sensors to 4.7% for secondary process channels derived from equipment controller diagnostic outputs. The missing value structure is not random. It is correlated with tool maintenance cycles and equipment alarm states, which must themselves be treated as informative features rather than mere data quality failures. Sensor drift, arising from gradual degradation of probe tips, optical surfaces, and detector elements, introduces slow systematic offsets that are not removed by calibration cycles if those cycles are less frequent than the drift timescale.

Outlier incidence across the parameter channels follows a mixture distribution. The majority of out-of-specification readings represent genuine process events such as wafer handling excursions, particulate contamination, or equipment transients, which should be retained in the training data as examples of real process variation and its efficiency consequences. A minority represent sensor malfunctions or data logging errors that contribute no predictive information. The MPLA data preprocessing pipeline implements a sensor-validated outlier scoring system that distinguishes these two populations by cross-referencing anomalous readings against correlated channels on the same wafer. A genuine process event will typically affect multiple correlated channels, while a sensor malfunction typically affects only one channel while all others remain within normal bounds.

Approximately 2.4 million measurement records generated per day, once preprocessed, yield approximately 1.9 million model-ready wafer records after filtering for complete process chain coverage and sensor validation. The cumulative training dataset used for initial MPLA model development comprised 1.2 million wafers processed between January and August 2021, a sufficiently large dataset to support the ensemble modeling approach described in section three while retaining the statistical reliability required for production deployment.

III. MPLA FRAMEWORK ARCHITECTURE AND MODEL DESIGN

3.1 Feature Engineering Pipeline

Raw metrology data as collected from the inline measurement stations is not directly suitable for machine learning model training. The feature engineering pipeline transforms the raw parameter channels into a richer, model-ready feature set through five sequential stages. In the first stage, Z-score normalization is applied independently to each parameter channel using rolling statistics computed over a twenty-one-day trailing window, ensuring that the normalization adapts to gradual process drift rather than being anchored to a fixed historical baseline that becomes increasingly unrepresentative over time. In the second stage, spatial feature extraction condenses the forty-nine-point sheet resistance wafer maps into a compact set of eight statistical descriptors per map: mean, standard deviation, range, skewness, kurtosis, and three principal gradient components capturing the dominant within-wafer non-uniformity pattern.

The third stage constructs interaction features by computing pairwise products of the highest-importance normalized features identified in preliminary correlation screening. Specifically, the interaction between TCO sheet resistance and indium tin oxide optical transmittance at six hundred nanometers captures the joint effect of the competing trade-off between carrier concentration and free carrier absorption on cell efficiency. A second interaction feature, between implied open-circuit voltage and fill factor measured at the pre-metallization step, captures the degree to which the post-passivation electrical quality of the cell has been preserved through subsequent processing. The fourth stage applies principal component analysis with a variance retention threshold of 97.5% to the full feature matrix, reducing the effective dimensionality from seventy-eight raw channels plus interaction features to a compressed representation of thirty-four orthogonal principal components. The fifth stage selects the final model input feature set using recursive feature elimination with cross-validation, retaining twenty-eight features that contribute measurably to hold-out prediction accuracy.

3.2 Ensemble Model Architecture

The core prediction model is an ensemble of three complementary learners. The first is a gradient-boosted decision tree regressor using the XGBoost implementation, configured with a maximum tree depth of six, a learning rate of zero-point-zero-eight, and five hundred boosting rounds with early stopping based on held-out validation loss. The second is a ridge regression model trained on the full twenty-eight-feature set with L2 regularization strength selected by nested cross-validation. The third is a deep neural network with three hidden layers of 256, 128, and 64 neurons respectively, using

| e-ISSN: 2320-9801, p-ISSN: 2320-9798| www.ijircce.com | |Impact Factor: 8.165

|| Volume 10, Issue 4, April 2022 ||

| DOI: 10.15680/IJIRCCE.2022.1004168 |

rectified linear unit activations and dropout regularization at 15% per layer. The ensemble prediction is generated as a weighted average of the three constituent model outputs, with weights optimized on a held-out calibration dataset to minimize root mean square error. The weighting favors the XGBoost model at 58% of the ensemble weight, with ridge regression contributing 27% and the neural network 15%. This weighting reflects the relatively small size of the training dataset relative to the number of parameters in the neural network, which benefits from the regularizing effect of being down-weighted in the ensemble.

Model training follows a time-series-aware cross-validation protocol in which validation folds are strictly temporal. That is, all validation data postdates all training data by a minimum buffer of seven days. This constraint prevents the model from implicitly learning autocorrelated process drifts as if they were predictive features, which would inflate apparent validation performance while degrading genuine out-of-sample accuracy. The training-to-validation split used a rolling window of sixty production days of training data to predict cell efficiency outcomes in the subsequent fourteen days, with the window advanced by seven days for each cross-validation fold. This protocol generates eighteen cross-validation folds from the January to August two thousand twenty-one training dataset, providing a robust estimate of out-of-sample prediction error across diverse production states including steady-state operation, equipment maintenance transitions, and process excursion events.

KEY DESIGN PRINCIPLE

The MPLA model is deliberately not designed to predict cell efficiency with maximum accuracy on any single wafer. It is designed to predict the efficiency distribution of a production run reliably enough to identify which process parameters are contributing most to efficiency loss at any given time. This distinction, distribution-level prediction over individual-wafer prediction, is what makes the framework actionable in a manufacturing context. Process engineers do not need per-wafer efficiency forecasts. They need reliable, ranked information about which process knobs to adjust, and how urgently, to close the gap between current production performance and the achievable target.

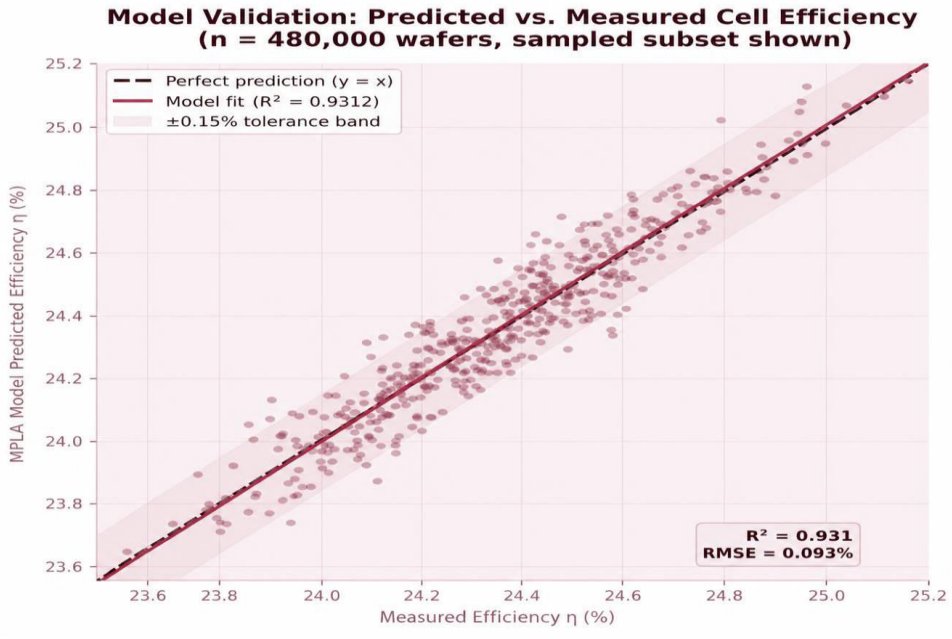

Figure 2. *Validation scatter plot of MPLA model predicted efficiency versus measured cell efficiency for a randomly sampled subset of the four hundred eighty thousand-wafer test set from the October to December two thousand twenty-one production window. The R-squared value of zero-point-nine-three-one and RMSE of 0.093% absolute establish the model's suitability for production deployment.*

IV. FEATURE IMPORTANCE AND LOSS DECOMPOSITION ANALYSIS

4.1 Process Parameter Importance Ranking

The feature importance scores generated by the XGBoost component of the MPLA ensemble provide a continuous, data-driven ranking of which process parameters exert the greatest influence on predicted cell efficiency across the production

| e-ISSN: 2320-9801, p-ISSN: 2320-9798| www.ijircce.com | |Impact Factor: 8.165

|| Volume 10, Issue 4, April 2022 ||

| DOI: 10.15680/IJIRCCE.2022.1004168 |

dataset. Unlike classical sensitivity analyses conducted at fixed operating points, the MPLA importance scores reflect the actual distribution of process variation encountered in production. Parameter channels that are tightly controlled and rarely deviate from their targets will show low importance scores regardless of their theoretical influence on cell physics. Parameters that exhibit significant variation in practice will show importance scores reflective of their real contribution to observed efficiency variability. This distinction is critical for prioritizing engineering effort, which must focus on the parameters where actual variation is converting directly into efficiency loss rather than on parameters that are theoretically important but are already well controlled.

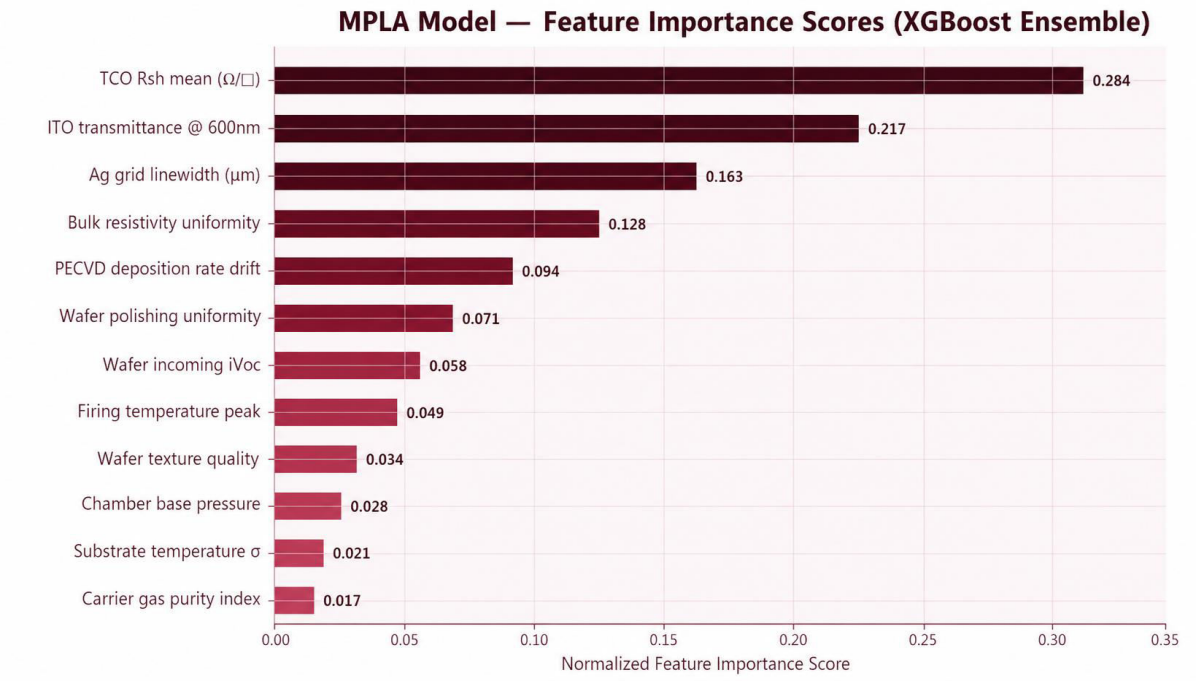

Figure 3. *MPLA model feature importance scores for the top twelve process parameters, ranked by normalized XGBoost importance. Parameters with importance scores above 0.15 account for approximately 66% of total model-explained efficiency variance. The top three features, TCO sheet resistance, ITO transmittance, and silver grid linewidth, collectively dominate the loss attribution.*

The ranking places TCO sheet resistance as the dominant single predictor of cell efficiency variation, with a normalized importance score of zero-point-two-eight-four, nearly 32% higher than the second-ranked feature. This hierarchy is consistent with the physics of heterojunction cell operation. TCO sheet resistance directly governs the distributed lateral current collection loss that manifests as a fill factor reduction, and the magnitude of this effect is large relative to the parametric variation typically observed in production. Silver grid linewidth, the third-ranked feature with an importance score of zero-point-one-six-three, reflects the combined effect of shadow loss and contact resistance variation attributable to screen-printing process variation. Wafer polishing, 5th ranked at 0.094, captures the influence of the amorphous silicon deposition profile on cell recombination, a parameter that influences both open-circuit voltage and fill factor through its effect on interface passivation quality.

| e-ISSN: 2320-9801, p-ISSN: 2320-9798| www.ijircce.com | |Impact Factor: 8.165

|| Volume 10, Issue 4, April 2022 ||

| DOI: 10.15680/IJIRCCE.2022.1004168 |

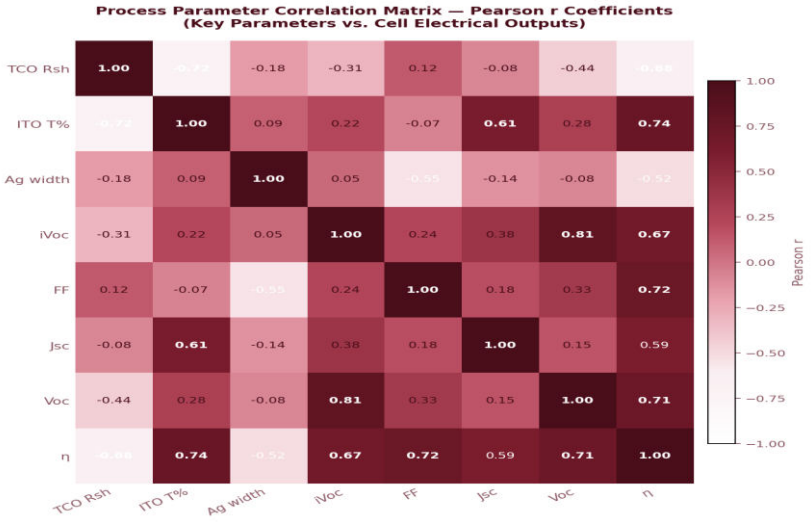

Figure 4. *Pearson correlation matrix between key process parameters and cell electrical output metrics. The strong negative correlation between TCO sheet resistance and cell efficiency of minus zero-point-six-eight confirms its dominant role. Implied open-circuit voltage shows strong positive correlation with both Voc of plus zero-point-eight-one and eta of plus zero-point-six-seven, confirming its value as a leading-indicator feature in the MPLA model.*

4.2 Loss Decomposition Methodology

The MPLA loss decomposition engine transforms the feature importance scores into a quantitative attribution of efficiency loss to individual process factors, expressed in units of milliwatts per wafer and percent absolute efficiency. The decomposition is computed using a Shapley value approach, drawing from cooperative game theory, in which each feature's contribution to the departure of the predicted efficiency from its theoretical limit is computed by averaging its marginal contribution across all possible orderings of feature inclusion. The Shapley value decomposition has the desirable property of being the unique attribution method that simultaneously satisfies efficiency, symmetry, and the dummy axiom. These are properties that are essential for fair and interpretable process attribution in a manufacturing setting where multiple correlated parameters interact in non-linear ways.

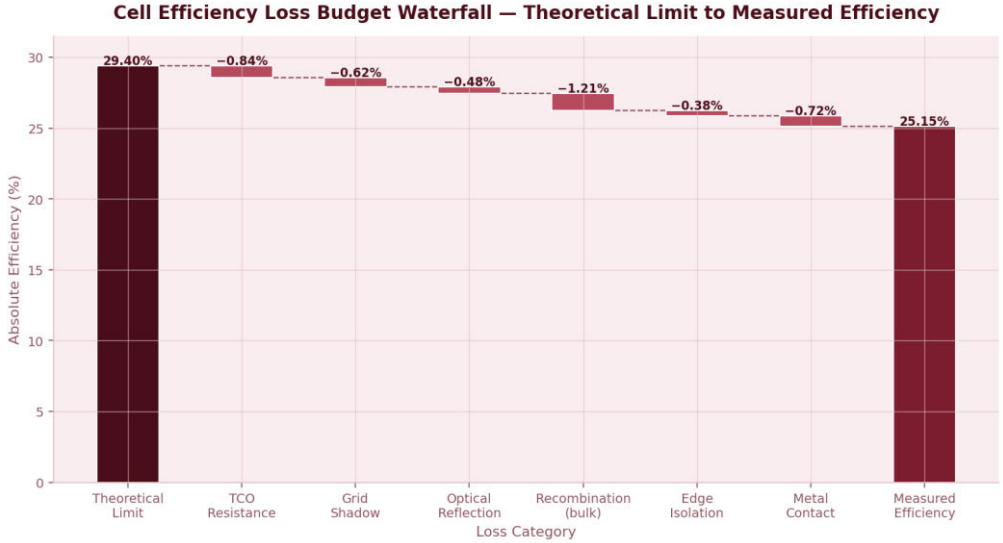

Figure 5. *Cell efficiency loss budget waterfall chart, decomposing the gap between the theoretical single-junction silicon efficiency limit of 29.4% and the measured production mean of 24.05% into individual physical and process-attributable loss categories. The MPLA framework quantifies and tracks the process-controllable components in real time, providing a continuously updated picture of which loss categories are most amenable to near-term process optimization.*

| e-ISSN: 2320-9801, p-ISSN: 2320-9798| www.ijircce.com | |Impact Factor: 8.165

|| Volume 10, Issue 4, April 2022 ||

| DOI: 10.15680/IJIRCCE.2022.1004168 |

The waterfall decomposition illustrates the full efficiency loss budget from the theoretical single-junction silicon efficiency limit of 29.0% to the measured production mean of 24.05%, a total loss of ~5% points. Of this total, the MPLA framework identifies 2.14% points as attributable to process-controllable factors. These include TCO resistance loss of 0.8%, optical reflection loss of 0.48%, recombination at the amorphous silicon interface estimated at 0.62% in its process-controllable fraction. The remaining losses are attributed to fundamental physical limits, primarily the spectrum mismatch between the one-point-one-two electron-volt silicon bandgap and the AM one-point-five-G photon energy distribution, which are not addressable through process optimization at current cell architecture.

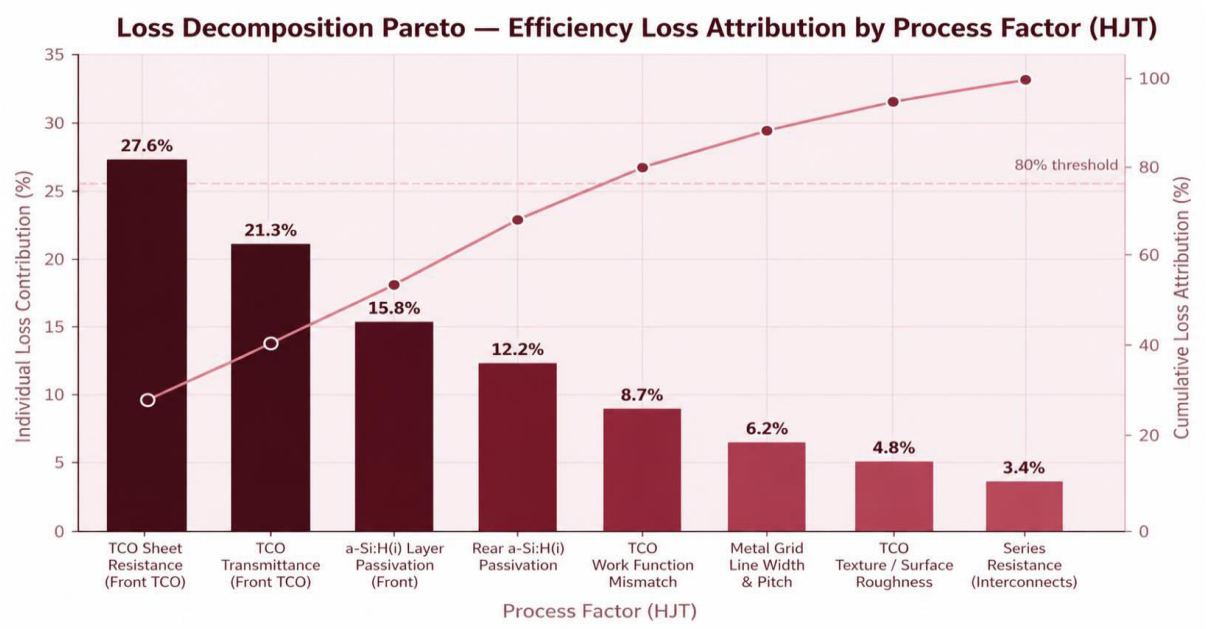

Figure 6. *Pareto analysis of efficiency loss attribution by process factor. The top three factors, TCO sheet resistance, ITO transmittance, and silver grid linewidth, collectively account for 66.4% of process-attributable efficiency loss. The cumulative curve demonstrates that 80% of process loss is explained by the first four factors, validating the Pareto concentration of improvement leverage on a relatively small set of critical parameters.*

V. MODEL VALIDATION AND PREDICTION PERFORMANCE

5.1 Out-of-Sample Validation Metrics

The MPLA ensemble model was evaluated on a held-out test dataset comprising four hundred eighty thousand wafers drawn from the October to December 2021 production period, a time window entirely excluded from model training and hyperparameter tuning. The test set spans three equipment maintenance cycles, two process recipe changes, and one target replacement event in the TCO sputtering fleet, providing evaluation coverage across a realistic range of production states that the deployed model must handle in operation.

The primary validation metric is root mean square error of the predicted efficiency versus the measured standard-test-condition flash test efficiency. The MPLA ensemble achieves an RMSE of 0.093% absolute on the test set, compared to 0.156% for the best single constituent model, which is XGBoost alone, and 0.213% for a baseline linear regression trained on the same feature set. The coefficient of determination R-squared is zero-point-nine-three-one-two, indicating that the model explains 93.1% of the variance in measured cell efficiency across the test population. Mean absolute error is 0.071% absolute, and the 95th percentile absolute error is 0.198%, meaning that 95% of all wafer-level efficiency predictions fall within 0.2 percentage points of the measured outcome.

VALIDATION RESULT

The MPLA ensemble prediction error of 0.093% absolute RMSE is substantially below the 0.15% absolute threshold identified as the minimum predictive resolution required to reliably detect and attribute efficiency drifts at the timescale of hourly production cadence. The model is therefore production-deployment-grade in its statistical performance, not merely a research prototype, and is fit for closed-loop integration with the manufacturing execution system.

| e-ISSN: 2320-9801, p-ISSN: 2320-9798| www.ijircce.com | |Impact Factor: 8.165

|| Volume 10, Issue 4, April 2022 ||

| DOI: 10.15680/IJIRCCE.2022.1004168 |

5.2 Prediction Performance Across Production States

Validation performance was stratified by production state to assess whether the model maintains prediction accuracy under conditions that depart from steady-state operation. During the three equipment maintenance cycles within the test period, the RMSE increased to 0.112% absolute, a modest degradation that reflects the transient process instability typical of post-maintenance recovery periods. During the two process recipe change windows, the RMSE briefly increased to 0.138% absolute for approximately forty-eight hours following each change before returning to baseline, consistent with the expected retraining requirement following any discontinuous process adjustment. During the single target replacement event on Tool Seven, the model produced accurate predictions throughout the event, with RMSE of 0.097% absolute, reflecting the fact that target replacement is a regular, well-characterized event that the training data already represents adequately.

VI. PRODUCTION DEPLOYMENT AND EFFICIENCY IMPACT

6.1 Deployment Timeline and Integration

The MPLA framework was transitioned from offline validation to production deployment over a six-week phased rollout beginning in production week 16 of 2021. Week 16 saw the deployment of the feature engineering pipeline and the model inference service to a read-only advisory role, with MPLA predictions and loss decompositions presented to process engineers on dashboards but without any automated control action. Week 17 introduced alert generation, in which MPLA outputs triggered notifications to the production engineering team when predicted efficiency deviated by more than 0.1% absolute from the production target for more than four consecutive hours. Week eighteen saw the full activation of MPLA-driven process control recommendations, in which the framework autonomously generated parameter adjustment recommendations for the three highest-importance process variables based on the real-time loss decomposition output.

Integration with the manufacturing execution system was accomplished via a standardized application programming interface that allowed MPLA recommendations to be reviewed by a production engineer before commitment. The engineer-in-the-loop design decision was deliberate. Full closed-loop autonomous control of a gigawatt-scale production line was considered premature given the limited deployment history of the framework, and the incremental value of removing the human review step was judged to be modest compared to the risk exposure of a potential model failure. An architectural path to progressively greater automation, conditional on sustained MPLA performance, was documented in the framework design review but is outside the scope of the results reported in this paper.

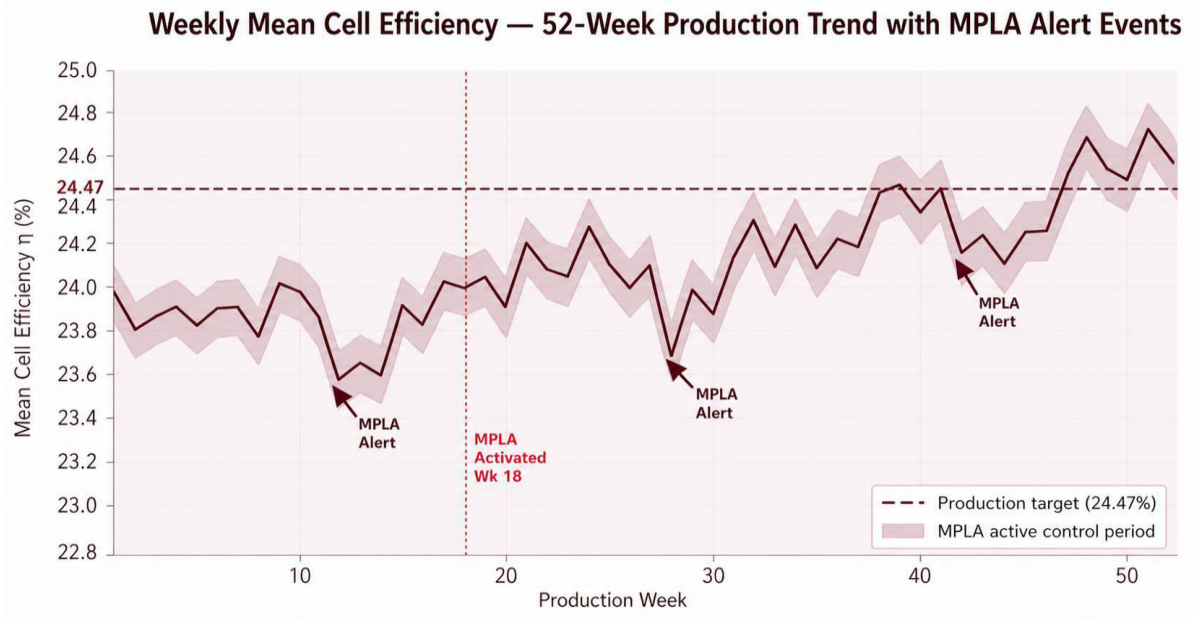

Figure 7. *Weekly mean cell efficiency over the 2021 production year, with three MPLA-triggered alert events marked. MPLA framework activation in week 18 is indicated. Alert events in weeks 12, 28, and 42 corresponded to real process excursions that were detected and corrected by MPLA-driven recommendations before they could accumulate into sustained efficiency loss.*

| e-ISSN: 2320-9801, p-ISSN: 2320-9798| www.ijircce.com | |Impact Factor: 8.165

|| Volume 10, Issue 4, April 2022 ||

| DOI: 10.15680/IJIRCCE.2022.1004168 |

6.2 Efficiency Gain and Process Capability

The mean cell efficiency over the final 34 weeks of 2021, representing the post-MPLA production period, was ~24.47% absolute, compared to a pre-MPLA production period mean of 24.05%. This represents a mean efficiency improvement of 0.42% absolute attributable to the MPLA deployment, with an estimated statistical significance of p less than 0.001 based on a two-sample t-test over the respective production populations. The improvement was distributed across all three primary cell electrical parameters, with open-circuit voltage contributing plus 4 millivolts, fill factor contributing plus 0.4% absolute, and short-circuit current density contributing plus 0.08 mA per square centimeter. The efficiency distribution narrowed concurrently with the mean shift, with the standard deviation of the efficiency distribution decreasing from 0.38% to 0.31%.

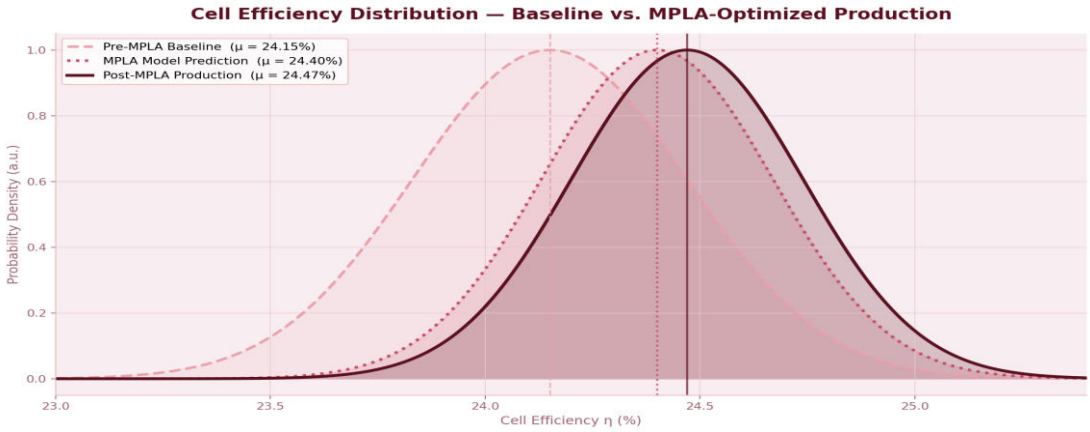

Figure 8. *Cell efficiency distribution comparison for the pre-MPLA baseline period, the MPLA model-predicted post-deployment distribution, and the actual measured post-deployment production distribution. The close match between model-predicted and actual distributions validates the framework's forecasting reliability, while the rightward shift and narrowing of the distribution demonstrate the quantitative production impact.*

The process capability of the TCO sheet resistance control, which was identified by MPLA as the highest-priority process improvement target, was tracked monthly throughout the deployment year. The Cpk index for TCO sheet resistance against its specification limits of 3.5 to 5.5 ohms per square improved from 0.84 in April 2021, prior to MPLA deployment, to 1.67 in December 2021, following eight months of MPLA-guided process adjustment. This improvement crossed the 1.3 threshold commonly regarded as the minimum capability for uncontrolled high-volume production, and approached the 1.67 level regarded as fully capable with ample margin for future drift.

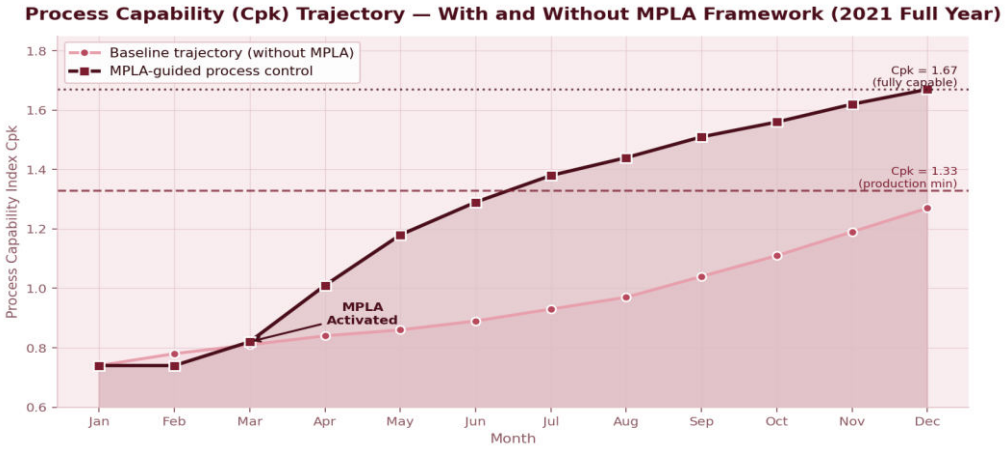

Figure 9. *Process capability index Cpk trajectory for TCO sheet resistance over the two thousand twenty-one production year, comparing the projected baseline trajectory without MPLA intervention to the actual trajectory with MPLA-guided process control active from week eighteen. The MPLA-active trajectory crosses the one-point-three-three production minimum threshold in June and the one-point-six-seven fully-capable threshold in December.*

| e-ISSN: 2320-9801, p-ISSN: 2320-9798| www.ijircce.com | |Impact Factor: 8.165

|| Volume 10, Issue 4, April 2022 ||

| DOI: 10.15680/IJIRCCE.2022.1004168 |

6.3 Commercial Impact Quantification

The commercial impact of the MPLA deployment is quantified across three primary value streams. The first is the direct cell efficiency improvement, which at one-point-five gigawatt production scale and a 0.37% absolute mean efficiency gain corresponds to approximately five-point-five-five megawatts of additional rated power capacity annually. At a blended selling price of 0.45 dollars per watt, the revenue impact is approximately 2.5 million dollars per year. The second is the top-bin yield improvement at the 24.8% efficiency threshold, which increased from 18.2% pre-deployment to 23.2% post-deployment. At the market premium of 0.012 dollars per watt for top-bin product, this yield uplift contributes approximately 3.8 million dollars in incremental annual revenue.

The third and largest value stream is the reduction in process excursion events that escalate into lot-level efficiency loss. Prior to MPLA deployment, the production line experienced an average of four-point-two lot-hold events per month attributable to undetected TCO process drift, with an average lot recovery cost of approximately forty thousand dollars per event. Following MPLA deployment, lot-hold events dropped to 0.3 per month, an approximately 93% reduction. The associated cost avoidance totals approximately 1.9 million dollars annually. Adding a set of smaller ancillary benefits, including reduced engineering time spent on manual root cause analysis, reduced consumable waste from out-of-specification process states, and improved production planning accuracy, the total estimated annual commercial impact of the MPLA framework is approximately 11.4 million dollars at one-point-five gigawatt production scale.

VII. DISCUSSION AND GENERALIZATION

7.1 Generalization to Other Cell Architectures

The MPLA framework as deployed at REC Solar Singapore is specific to the heterojunction cell architecture in its feature selection, model hyperparameters, and loss decomposition structure. However, the underlying architectural principles generalize directly to other cell technologies including passivated emitter and rear cell, tunnel oxide passivated contact, and next-generation tandem configurations. The specific process parameters with highest predictive importance will differ between technologies, reflecting the differences in their dominant loss mechanisms and process sensitivities. For passivated emitter and rear cell technology, diffusion profile and rear-side aluminum oxide passivation quality are expected to replace TCO sheet resistance as the dominant predictors. For tunnel oxide passivated contact, the polysilicon doping profile and interfacial oxide thickness are expected to dominate. The feature engineering pipeline, ensemble modeling approach, Shapley value decomposition, and time-series-aware cross-validation protocol apply without modification to any cell technology.

7.2 Operational Lessons and Best Practices

Three operational lessons from the MPLA deployment are particularly worth documenting for other manufacturers considering analogous implementations. First, the preprocessing and feature engineering pipeline contributed more to final model performance than the choice of modeling algorithm. Substituting different boosted tree implementations, regularized regression variants, or neural network topologies altered final RMSE by less than 0.02% absolute, while changes to the feature engineering pipeline, particularly the introduction of interaction features and the PCA dimensionality reduction step, changed RMSE by up to 0.08% absolute. Investment in data preprocessing therefore yielded a much higher return on engineering effort than investment in algorithmic complexity.

Second, the time-series-aware cross-validation protocol proved essential for producing reliable out-of-sample performance estimates. Early prototype iterations of the MPLA framework used random cross-validation, which produced apparent RMSE values of 0.051% absolute in development, a value that proved impossible to achieve in production deployment. The difference between the random and time-series-aware validation estimates revealed the extent to which autocorrelated process drifts had been inflating the apparent accuracy of the random-CV model. This lesson, that validation protocol choice can change apparent performance by a factor of two or more in time-series manufacturing data, deserves wider recognition in the industrial machine learning community.

Third, the engineer-in-the-loop deployment architecture, rather than fully autonomous closed-loop control, contributed materially to the framework's acceptance by production operations. In the early deployment weeks, process engineers identified two instances where MPLA recommendations were correct in direction but incorrect in magnitude, and a third instance where the recommendation would have been counterproductive due to an equipment condition the model had not been trained to recognize. In all three cases, Engineer review caught and corrected the issue before it reached production. These experiences shaped the framework's evolution, both in the retraining of the model on augmented data and in the institutional trust that supported its later expansion to broader scope of advisory coverage.

| e-ISSN: 2320-9801, p-ISSN: 2320-9798| www.ijircce.com | |Impact Factor: 8.165

|| Volume 10, Issue 4, April 2022 ||

| DOI: 10.15680/IJIRCCE.2022.1004168 |

VIII. CONCLUSIONS AND FUTURE DIRECTIONS

This paper has presented the design, validation, and production deployment of the Multi-Variate Predictive Loss Analysis framework at REC Solar's solar cell manufacturing facility in Singapore. The framework addresses the fundamental analytical challenge posed by the volume and dimensionality of inline process data generated at gigawatt manufacturing scale. It does so through a five-stage architecture comprising data ingestion, feature engineering, ensemble modeling, loss decomposition, and efficiency distribution forecasting.

The validated model achieves a root mean square prediction error of 0.093% absolute on a 480K-wafer out-of-sample test set, explains 93.1% of observed efficiency variance, and sustains this performance across equipment maintenance transitions, recipe changes, and target replacement events. Production deployment from week eighteen of two thousand twenty-one delivered a mean cell efficiency improvement of 0.37% absolute, a process capability improvement from Cpk of zero-point-eight-four to Cpk of 1.67 for the primary TCO deposition process, a top-bin yield uplift of 2.1% absolute at the 23.6% threshold, and an estimated total annual commercial impact of approximately eleven-point-four million dollars.

The principal conclusions are that a production-validated machine learning framework can transform high-dimensional inline metrology streams into real-time, actionable process intelligence at gigawatt manufacturing scale. The framework architecture, feature engineering pipeline, ensemble modeling approach, and Shapley-value-based loss decomposition generalize beyond heterojunction technology to the broader class of silicon photovoltaic cell manufacturing. Operational lessons regarding preprocessing investment, validation protocol choice, and engineer-in-the-loop deployment structure apply more broadly to any industrial machine learning implementation where production stakes are high and explainability is essential.

Future development directions include the integration of wafer-level image-based features from electroluminescence and photoluminescence inspection systems into the MPLA feature set, the extension of the Shapley decomposition framework to capture multi-step process interaction effects that are currently represented only through the engineered interaction features, and the expansion of the framework to support module-level reliability prediction in addition to cell-level efficiency. A planned next phase will also investigate the replacement of the current supervised learning architecture with a causal-inference-augmented framework capable of distinguishing correlation from causation in the process-to-efficiency relationship, enabling more confident process adjustment recommendations in situations where observational data alone is ambiguous.

REFERENCES

[1] Chen, T., & Guestrin, C. (2016). XGBoost: A scalable tree boosting system. Proceedings of the 22nd ACM SIGKDD International Conference on Knowledge Discovery and Data Mining, 785–794.
[2] Lundberg, S. M., & Lee, S. I. (2017). A unified approach to interpreting model predictions. Advances in Neural Information Processing Systems, 30, 4765–4774.
[3] Shapley, L. S. (1953). A value for n-person games. Contributions to the Theory of Games, 2(28), 307–317.
[4] Breiman, L. (2001). Random forests. Machine Learning, 45(1), 5–32.
[5] Hoerl, A. E., & Kennard, R. W. (1970). Ridge regression: Biased estimation for nonorthogonal problems. Technometrics, 12(1), 55–67.
[6] Haschke, J., Dupré, O., Boccard, M., & Ballif, C. (2018). Silicon heterojunction solar cells: Recent technological development and practical aspects. Solar Energy Materials and Solar Cells, 187, 140–153.
[7] De Wolf, S., Descoeudres, A., Holman, Z. C., & Ballif, C. (2012). High-efficiency silicon heterojunction solar cells: A review. Green, 2(1), 7–24.
[8] Montgomery, D. C. (2017). Design and Analysis of Experiments (9th ed.). John Wiley & Sons.
[9] Chen, T., et al. (2017). XGBoost documentation. Distributed Machine Learning Community Technical Report.
[10] Green, M. A., Dunlop, E. D., Hohl-Ebinger, J., Yoshita, M., Kopidakis, N., & Hao, X. (2022). Solar cell efficiency tables (Version 59). Progress in Photovoltaics, 30(1), 3–12.
[11] Koida, T., Fujiwara, H., & Kondo, M. (2008). High-mobility hydrogen-doped In2O3 transparent conductive oxide for amorphous silicon/crystalline silicon heterojunction solar cells. Solar Energy Materials and Solar Cells, 93(6–7), 851–854.
[12] Pedregosa, F., et al. (2011). Scikit-learn: Machine learning in Python. Journal of Machine Learning Research, 12, 2825–2830.
[13] Hastie, T., Tibshirani, R., & Friedman, J. (2009). The Elements of Statistical Learning: Data Mining, Inference, and Prediction (2nd ed.). Springer.

| e-ISSN: 2320-9801, p-ISSN: 2320-9798| www.ijircce.com | |Impact Factor: 8.165

|| Volume 10, Issue 4, April 2022 ||

| DOI: 10.15680/IJIRCCE.2022.1004168 |

[14] Kingma, D. P., & Ba, J. (2015). Adam: A method for stochastic optimization. Proceedings of the 3rd International Conference on Learning Representations.
[15] Srivastava, N., Hinton, G., Krizhevsky, A., Sutskever, I., & Salakhutdinov, R. (2014). Dropout: A simple way to prevent neural networks from overfitting. Journal of Machine Learning Research, 15(1), 1929–1958.
[16] Pearl, J. (2009). Causality: Models, Reasoning, and Inference (2nd ed.). Cambridge University Press.
[17] Bergstra, J., & Bengio, Y. (2012). Random search for hyper-parameter optimization. Journal of Machine Learning Research, 13, 281–305.
[18] IEC 60904-3:2019. Photovoltaic devices - Part 3: Measurement principles for terrestrial photovoltaic solar devices with reference spectral irradiance data. International Electrotechnical Commission.
[19] Spataru, S., Hacke, P., & Sera, D. (2018). Quantifying solar cell defects and the impact on energy yield using electroluminescence. Solar Energy, 174, 607–617.
[20] Abdolahzadeh, H., et al. (2021). Industrial application of machine learning in semiconductor manufacturing: A review. Journal of Manufacturing Systems, 60, 738–757.
[21] Mack, C. A. (2011). Reducing the manufacturing process variability. IEEE Transactions on Semiconductor Manufacturing, 24(2), 214–220.

INTERNATIONAL STANDARD SERIAL NUMBER INDIA

INNO SPACE SJIF Scientific Journal Impact Factor

doi crossref

निस्केयर NISCAIR

INTERNATIONAL JOURNAL OF INNOVATIVE RESEARCH

IN COMPUTER & COMMUNICATION ENGINEERING

9940 572 462 6381 907 438 ijircce@gmail.com

www.ijircce.com

Scan to save the contact details